Nonlinear Vertical Oscillations of a Particle in a Sheath of a rf Discharge

A. V. Ivlev,* R. Sütterlin, V. Steinberg,† M. Zuzic, and G. Morfill
Max-Planck-Institut für Extraterrestrische Physik, D-85740 Garching, Germany
(Received 30 March 2000)

A new simple method to measure the spatial distribution of the electric field in the plasma sheath is proposed. The method is based on the experimental investigation of vertical oscillations of a single particle in the sheath of a low-pressure radio-frequency discharge. It is shown that the oscillations become strongly nonlinear as the amplitude increases. The theory of anharmonic oscillations provides a good quantitative description of the data and gives estimates for the first two anharmonic terms in an expansion of the sheath potential around the particle equilibrium.

PACS numbers: 52.25.Zb, 52.25.Gj, 52.35.–g, 52.80.Pi

There are various experimental methods on the plasma sheath diagnostic in low-pressure gas discharges (see, e.g., [1–3], and references therein). Most of the methods are based on optical emission spectroscopy and temporally resolved probe measurements and are rather complicated technically. We propose an "alternative" simple method to measure the spatial distribution of the electric field in the plasma sheath based on investigation of "large-amplitude" vertical oscillations of micron sized particles.

So far, investigation of the particle oscillations in the sheath of a radio-frequency (rf) discharge was one of the methods used to determine the particle charge [4,5]. This method is based on the assumption that the vertical distribution of the sheath potential can be approximated by a parabolic profile [6], so that the oscillations are always harmonic. This assumption is reasonable for sufficiently high gas pressure, when the mean free path of ions is much less than the vertical spatial scale of the sheath field [6]: For example, the model of a parabolic rf sheath in an argon plasma can be applied for pressures above $\simeq 20$ Pa. But for $p \lesssim 10$ Pa the sheath profile might deviate strongly from a parabolic one. In this case, the oscillations are harmonic only if their amplitude is very small.

In this Letter, we report experimental and theoretical investigations of nonlinear (large-amplitude) vertical oscillations of a single particle in the sheath of a low-pressure rf discharge. Comparing the experimental results to the theory of anharmonic oscillations we estimate the first two anharmonic terms in an expansion of the sheath potential around the particle equilibrium height. This allows us to reconstruct the distribution of the vertical electric field in the wide region of the sheath.

Experimental setup and results.—The experiments are performed in a so-called Gaseous Electronic Conference rf reference cell [7] with the electrode system modified as shown in Fig. 1. The lower aluminum electrode, 230 mm in diameter, is capacitively coupled to a rf generator providing a peak-to-peak voltage $\simeq 70$ V (rf power $\simeq 2$ W). A ring-shaped upper grounded electrode with an outer diameter of 200 mm and a thickness of 10 mm is located 50 mm above the lower electrode. A 2 mm thick copper ring with a 40 mm inner diameter is placed on the lower electrode to confine the particle above the center. Argon gas at a pressure of 0.5 Pa is used for the discharge. For this pressure, a self-bias voltage $\simeq -33$ V on the lower electrode provides the sheath with a (visible) thickness of $\simeq 20$ mm and causes a spherical polystyrene particle (density 1.05 g/cm^3, diameter 7.6 ± 0.1 μm) to levitate $\simeq 14$ mm above the electrode.

At a height 8 mm above the lower electrode a horizontal wire of 0.5 mm diameter and 80 mm length is placed directly below the levitated particle. A low-frequency sinusoidal voltage of amplitude U_{ex} is applied to this wire to excite the vertical oscillations of the particle. The frequency $\omega/2\pi$ of the voltage was varied from 0.1 up to 40 Hz and back in 0.1 Hz steps. To determine the oscillation amplitude, we illuminated the particle with a vertical laser sheet of $\simeq 140$ μm thickness and imaged it from the side by an external digital charge-coupled device camera (maximum field rate is 50 fields/s; resolution is 768×576 pixels).

For small excitation voltage ($U_{ex} \lesssim 30$ mV), we observed the usual linear (harmonic) oscillations: The amplitude has a single symmetric narrow maximum at the resonance frequency $\omega_0/2\pi \simeq 17.0$ Hz (primary resonance). However, for larger U_{ex} the dependence clearly exhibits nonlinearity (see, e.g., [8]). Compare Figs. 2(a) and 2(b) for $U_{ex} = 100$ and 200 mV: When ω increases [Fig. 2(a)], the amplitude grows continuously until a certain frequency (ω_+) is reached; then it "jumps"

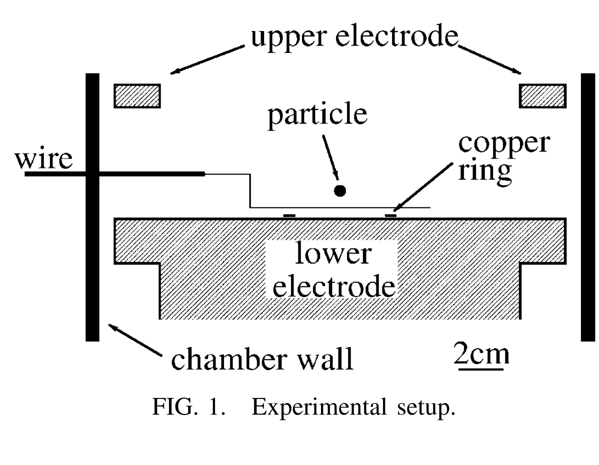

FIG. 1. Experimental setup.

 0031-9007/00/85(19)/4060(4)$15.00

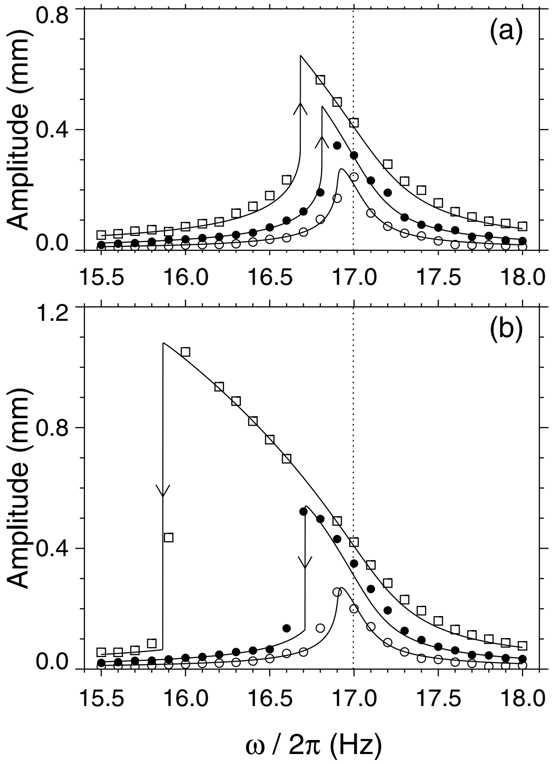

FIG. 2. Variation of the amplitude of particle oscillations close to the primary resonance for increasing (a) and decreasing (b) frequency of excitation, ω, and for different magnitudes of the excitation voltage U_{ex}: 50 mV (open circles), 100 mV (closed circles), and 200 mV (squares). Solid lines show the least-squares fit of the points using Eq. (4) for a. The vertical dotted line indicates the position of the resonance frequency, ω_0, obtained from the fit.

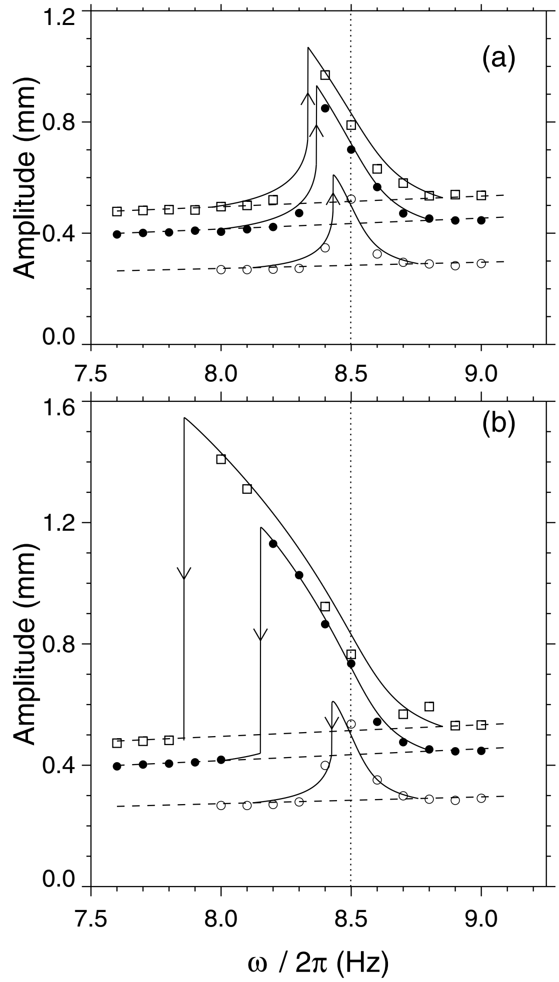

FIG. 3. Variation of the amplitude of particle oscillations close to the superharmonic resonance for increasing (a) and decreasing (b) frequency of excitation, ω, and for different magnitudes of the excitation voltage U_{ex}: 4 V (open circles), 6 V (closed circles), and 7 V (squares). Solid lines show the least-squares fit of the points using Eq. (6) for a_2. The tilted dashed lines represent the linear amplitude offset a_1. The vertical dotted line indicates the position of the half resonance frequency, $\frac{1}{2}\omega_0$, obtained from the fit.

upward and thereafter decreases monotonically as ω is further increased. On the "way back" [Fig. 2(b)], the amplitude grows continuously until another frequency (ω_-) is reached. Then it spontaneously jumps downward and continues to decrease as ω is reduced further. We found that ω_+ is always larger than ω_-. Outside this "hysteresis zone," the experimental points obtained for increasing and decreasing frequencies practically overlap. The shift of the maximum, as well as the width of the hysteresis zone rapidly increases with U_{ex}.

Another peculiarity of the oscillations is the secondary resonances—two maxima at $\omega \simeq \frac{1}{2}\omega_0$ and $\omega \simeq 2\omega_0$, which are observed for sufficiently high U_{ex}. Figure 3 shows the peak in the vicinity $\omega \simeq \frac{1}{2}\omega_0$ (superharmonic resonance) for different values of U_{ex}. There is a finite offset with some slope (marked by the dashed line), which represents the low-frequency tail of the primary resonance. The shape of the peaks resembles that of the primary resonance. In contrast, for the subharmonic resonance at $\omega \simeq 2\omega_0$ (Fig. 4) the behavior is qualitatively different. When U_{ex} is below a certain threshold, we see only the offset—the high-frequency tail of the primary resonance. However, when U_{ex} exceeds this threshold a peak appears with an amplitude which increases monotonically with U_{ex}. With increasing ω [Fig. 4(a)] we found that a jump in amplitude occurs at some ω_*, followed by a rapid decrease back to the offset. For decreasing ω [Fig. 4(b)], the amplitude follows the same resonance curve down to ω_*, but then for $\omega < \omega_*$, the amplitude increases continuously until the particle is ejected from the sheath.

Theory and discussion.—The particle oscillations are determined by the spatial distribution of the electrostatic potential, $\phi(z)$, in the sheath. Without excitation, a particle is levitated in the minimum of the potential well ($z = 0$), where the gravitational force, Mg, is balanced by the electrostatic force, $Q(0)E(0) \equiv Q_0E_0$. We assume that the equilibrium particle charge, $Q(z)$, changes weakly with z [compared to the electric field of

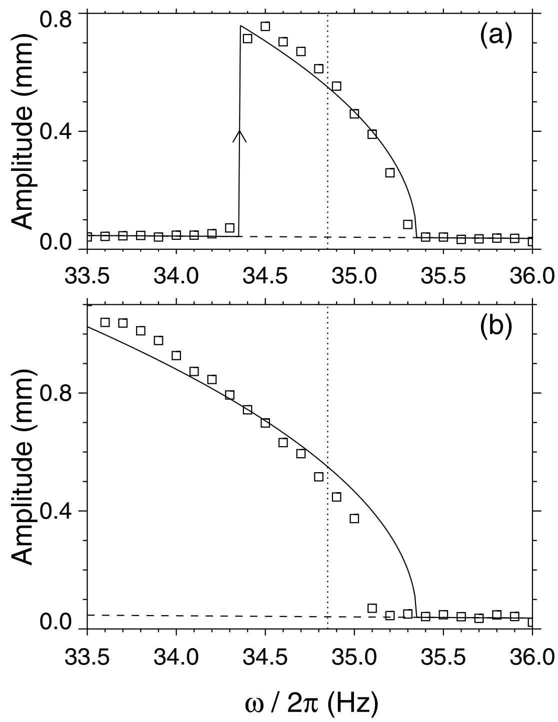

FIG. 4. Variation of the amplitude of particle oscillations close to the subharmonic resonance for increasing (a) and decreasing (b) frequency of excitation, ω. The excitation voltage $U_{ex} = 2$ V. Solid lines show the least-squares fit of the points using Eq. (8) for a_2. The tilted dashed lines represent the linear amplitude offset a_1. The vertical dotted line indicates the position of the double resonance frequency, $2\omega_0$, obtained from the fit.

the sheath, $E(z)$], so that we can set $Q \simeq Q_0 =$ const. The particle collision experiments [9] in Ar discharge at pressures $p \sim 1$ Pa confirm this assumption: Typically, the spatial scale of the field change is approximately 1 order smaller than that of the charge change [10]. The electrostatic energy of the particle, $\mathcal{U} = Q\phi$, can be expanded around $z = 0$ in the series $\mathcal{U}(z) = \mathcal{U}_0' z + \frac{1}{2}\mathcal{U}_0'' z^2 + \frac{1}{6}\mathcal{U}_0''' z^3 + \frac{1}{24}\mathcal{U}_0^{(4)} z^4 + O(z^5)$. Using the equilibrium condition $Mg = QE_0 \equiv -\mathcal{U}_0'$ and the definition of the resonance frequency, $M\omega_0^2 = -QE_0' \equiv \mathcal{U}_0''$, we rewrite it as follows:

$$\mathcal{U}(z) \simeq M(-gz + \tfrac{1}{2}\omega_0^2 z^2 + \tfrac{1}{3}\alpha z^3 + \tfrac{1}{4}\beta z^4), \quad (1)$$

where $\alpha = \mathcal{U}_0'''/2M$ and $\beta = \mathcal{U}_0^{(4)}/6M$ are the anharmonic coefficients. Keeping only the first two anharmonic coefficients is (in practice) sufficient to describe all major peculiarities of a nonlinear oscillator [8,11]. Using Eq. (1), we obtain the equation for the particle oscillation,

$$\ddot{z} + 2\gamma\dot{z} + \omega_0^2 z + \alpha z^2 + \beta z^3 = \frac{F(z)}{M}\cos\omega t. \quad (2)$$

Here γ is the damping rate due to neutral gas friction; F is the excitation force acting from the wire. This force presumably depends on the vertical position of the particle, and we expand it up to quadratic terms, $F(z) \simeq F_0 + F_0' z + \frac{1}{2}F_0'' z^2$.

First, let us consider the primary resonance $\omega \simeq \omega_0$. Nonlinear effects are stronger when the oscillation amplitude is larger, and therefore we are interested in a narrow region $\epsilon = \omega - \omega_0$ around the resonance frequency, where $|\epsilon| \ll \omega_0$. This approach is normally valid in the limit $\gamma \ll \omega_0$ and is justified for our case: The calculated $\gamma/2\pi \simeq 0.068$ Hz (see [12]) is much less than the measured $\omega_0/2\pi \simeq 17.0$ Hz. Then, we obtain from Eq. (2),

$$\ddot{z} + 2\gamma\dot{z} + \omega_0^2 z + \alpha z^2 + \beta z^3 = \omega_0^2 A\cos(\omega_0 + \epsilon)t, \quad (3)$$

where $A = F_0/M\omega_0^2 \equiv kU_{ex}$ and k is a "scale factor" of the oscillation amplitude. In Eq. (3) we omit the higher order terms in $F(z)$, because for the primary resonance they are not important when the inequality $A|F_0'/F_0| \ll 1$ is satisfied (this condition always holds in our case). In accordance with the method of successive approximations for anharmonic oscillations [8,11], the first term in the solution of Eq. (3) is $z(t) \simeq a\cos(\omega_0 + \epsilon)t$, and the dependence of the amplitude a on ϵ and A is given by

$$a^2[(\epsilon - \kappa a^2)^2 + \gamma^2] = \tfrac{1}{4}\omega_0^2 A^2, \quad (4)$$

where $\kappa = 3\beta/8\omega_0 - 5\alpha^2/12\omega_0^3$ characterizes a nonlinear shift of the primary resonance frequency. The least-squares fit of the experimental points for the low-amplitude (linear) primary resonance yields the resonance frequency $\omega_0/2\pi = 17.0$ Hz, the damping rate $\gamma/2\pi = 0.067$ Hz, and the amplitude scale factor $k = 0.042$ mm/V (note that the fitted damping rate is very close to $\gamma/2\pi = 0.068$ Hz evaluated from the theory [12]). Using these values, we fit the points for the nonlinear oscillations in Fig. 2 to the function $a(\epsilon, A)$ from Eq. (4). The solid lines represent the least-squares fit with $\kappa/2\pi = -0.96$ Hz/mm^2. If each curve is fitted independently, this value varies within 5%. The hysteresis appears when A exceeds the critical value: $A_{cr}^2 = \frac{32}{3\sqrt{3}}(\gamma^3/|\kappa|\omega_0^2) \simeq (2.4 \times 10^{-3}$ mm$)^2$, which corresponds to $U_{ex} \simeq 60$ mV.

Second, for the superharmonic resonance $\omega \simeq \frac{1}{2}\omega_0$, we set $\epsilon = \omega - \frac{1}{2}\omega_0$. The solution of Eq. (2) is approximately a sum of the first- and second-order terms [8], $z(t) \simeq z_1(t) + z_2(t)$. The first (linear) term is $z_1(t) = a_1\cos(\frac{1}{2}\omega_0 + \epsilon)t$, where $a_1 \simeq \frac{4}{3}(1 + \frac{4}{3}\epsilon/\omega_0)A$ represents the amplitude offset (dashed line in Fig. 3), and z_2 describes the nonlinear resonance peak. Substituting the expression for $z_1(t)$ in Eq. (2), we get the resonance terms $z_1^2 \propto \cos(\omega_0 + 2\epsilon)t$ in the resulting equation for z_2 (see Ref. [8]). Retaining these terms, we obtain

$$\ddot{z}_2 + 2\gamma\dot{z}_2 + \omega_0^2 z_2 + \alpha z_2^2 + \beta z_2^3 = -\tfrac{8}{9}\alpha_{(\omega/2)}A^2\cos(\omega_0 + 2\epsilon)t, \quad (5)$$

where $\alpha_{(\omega/2)} = \alpha - \frac{3}{4}\omega_0^2/\ell$ and $\ell = F_0/F_0' < 0$ is the spatial scale of change of the excitation force. In Eq. (5)

we omit the small terms $O(A^2/\ell^2)$. Formally, Eq. (5) is similar to that for the primary resonance [see Eq. (3)], and therefore shapes of the corresponding curves are qualitatively the same. Assuming $z_2(t) \simeq a_2 \cos(\omega_0 + 2\epsilon)t$, we obtain for the superharmonic resonance,

$$a_2^2[(2\epsilon - \kappa a_2^2)^2 + \gamma^2] = \frac{16}{81}\left(\frac{\alpha_{(\omega/2)}}{\omega_0}\right)^2 A^4. \tag{6}$$

The independent least-squares fit of the experimental points in Fig. 3 using Eq. (6) gives for each curve values of ω_0 and γ, which are nearly the same as those for the primary resonance (deviation within $\simeq 0.5\%$), $\kappa/2\pi = -1.0 \pm 5\%$ Hz/mm^2, and $|\alpha_{(\omega/2)}|/(2\pi)^2 = 32 \pm 10\%$ Hz^2/mm. The critical value of A for the hysteresis is $A_{\rm cr}^4 = \frac{9\sqrt{3}}{2}(\gamma^3\omega_0^2/|\kappa|\alpha_{(\omega/2)}^2) \simeq (0.14\text{ mm})^4$, which corresponds to $U_{\rm ex} \simeq 3.5$ V.

Third, for the subharmonic resonance $\omega \simeq 2\omega_0$, we set $\epsilon = \omega - 2\omega_0$. The first-order term is $z_1(t) = -a_1\cos(2\omega_0 + \epsilon)t$ with the amplitude offset $a_1 \simeq \frac{1}{3}(1 - \frac{4}{3}\epsilon/\omega_0)A$. Retaining the necessary terms (see Ref. [8]), we derive from Eq. (2) the equation for z_2,

$$\ddot{z}_2 + 2\gamma\dot{z}_2 + \omega_0^2[1 - \tfrac{2}{3}(\alpha_{(2\omega)}A/\omega_0^2)\cos(2\omega_0 + \epsilon)t]z_2 + \alpha z_2^2 + \beta z_2^3 = 0, \tag{7}$$

where $\alpha_{(2\omega)} = \alpha + \frac{3}{2}\omega_0^2/\ell$. We see that Eq. (7) is an equation of a nonlinear parametric oscillator, and therefore the subharmonic resonance appears due to a parametric instability [8]. Putting $z_2(t) \simeq a_2\cos(\omega_0 + \frac{1}{2}\epsilon)t$ we get

$$a_2^2[(\tfrac{1}{2}\epsilon - \kappa a_2^2)^2 + \gamma^2] = \frac{1}{36}\left(\frac{\alpha_{(2\omega)}}{\omega_0}\right)^2 A^2 a_2^2. \tag{8}$$

The solution of Eq. (8) has the following peculiarities [8]: If A is less than the threshold value $A_{\rm th} = 6\gamma\omega_0/|\alpha_{(2\omega)}|$, then Eq. (8) has only the zero solution $a_2 = 0$, and thus just the offset $a_1(\omega)$ can be observed. For sufficiently high $U_{\rm ex}$ ($A > A_{\rm th}$), a nonzero solution exists for $\epsilon_{\rm b1} < \epsilon < \epsilon_{\rm b2}$, where $\epsilon_{\rm b1,2} = \mp 2\gamma\sqrt{A^2/A_{\rm th}^2 - 1}$. The least-squares fit of the points in Fig. 4 ($U_{\rm ex} = 2.0$ V) with Eq. (8) gives us $\kappa/2\pi = -0.95$ Hz/mm^2 and $|\alpha_{(2\omega)}|/(2\pi)^2 = 320$ Hz^2/mm. Thus, $A_{\rm th} \simeq 0.02$ mm, which corresponds to $U_{\rm ex} \simeq 0.5$ V. The fit for the center $\epsilon = 0$ yields 34.85 Hz, which is $\simeq 2\%$ larger than the double value of ω_0 obtained for the primary and superharmonic resonance.

Finally we can reconstruct the sheath potential, $\phi(z)$. Using the fitted values $|\alpha_{(\omega/2)}| = |\alpha - \frac{3}{4}\omega_0^2/\ell| \simeq (2\pi)^2 \times 30$ Hz^2/mm and $|\alpha_{(2\omega)}| = |\alpha + \frac{3}{2}\omega_0^2/\ell| \simeq (2\pi)^2 \times 320$ Hz^2/mm, we evaluate the first anharmonic coefficient and the spatial scale of the excitation force: $\alpha/(2\pi)^2 \simeq -130$ Hz^2/mm and $\ell \simeq -2$ mm. With this value for α and $\kappa/2\pi = -0.95$ Hz/mm, we estimate the second anharmonic coefficient: $\beta/(2\pi)^2 \simeq 20$ Hz^2/mm^2. Then, using Eq. (1) we evaluate the potential energy of a particle in the sheath field (z in mm),

$$\begin{aligned}\mathcal{U}(z) &\simeq M\omega_0^2(-0.9z + \tfrac{1}{2}z^2 - \tfrac{1}{3}0.5z^3 + \tfrac{1}{4}0.07z^4) \\ &\propto \phi(z).\end{aligned} \tag{9}$$

We see that the first anharmonic term results in a significant deviation of the sheath potential from a parabolic one, and therefore the oscillations become strongly nonlinear when the amplitude reaches a few tenths of mm, or more. At the same time the obtained coefficients of the series converge rapidly, so that for $|z| \lesssim 2$ mm we can limit ourselves to expansion (1). Thus, Eq. (9) provides a convenient analytical expression for the electric field in a rather wide vicinity of the equilibrium particle position.

In this Letter, we have presented one example of nonlinear particle oscillations in the sheath of a low-pressure rf discharge and its quantitative analysis. The proposed simple method opens the possibility to retrieve the profile of the electric field in the wide region of the sheath, using particles of different masses (and thus levitating at different heights). Analysis for each particle allows us to reconstruct the electric field in a range of a few mm, and therefore it is sufficient to use just a few different particles to get a rather precise field distribution in the whole sheath range. Hence, we believe that experiments with excitation of nonlinear oscillations might be an effective way to study the sheath.

*Electronic address: ivlev@mpe.mpg.de.
†Present address: Department of Physics of Complex Systems, Weizmann Institute of Science, Rehovot 76100, Israel.

[1] U. Czarnetzki, D. Luggenhölscher, and H. F. Döbele, Plasma Sources Sci. Technol. **8**, 230 (1999).
[2] A. H. Sato and M. A. Lieberman, J. Appl. Phys. **68**, 6117 (1990).
[3] C. M. O. Mahony, R. Al Wazzan, and W. G. Graham, Appl. Phys. Lett. **71**, 608 (1997).
[4] A. Melzer, T. Trottenberg, and A. Piel, Phys. Lett. A **191**, 301 (1994).
[5] H. Schollmeyer *et al.,* Phys. Plasmas **6**, 2693 (1999).
[6] E. B. Tomme *et al.,* Phys. Rev. Lett. **85**, 2518 (2000).
[7] P. J. Hargis, Jr. *et al.,* Rev. Sci. Instrum. **65**, 140 (1994).
[8] L. D. Landau and E. M. Lifshitz, *Mechanics* (Pergamon, Oxford, 1960).
[9] U. Konopka, G. E. Morfill, and L. Ratke, Phys. Rev. Lett. **84**, 891 (2000).
[10] U. Konopka, Ph.D. thesis, Ruhr-Universität Bochum, 2000.
[11] A. H. Nayfeh and D. T. Mook, *Nonlinear Oscillations* (Wiley, New York, 1979).
[12] P. Epstein, Phys. Rev. **23**, 710 (1924).